ISSN 1070-3632, Russian Journal of General Chemistry, 2014, Vol. 84, No. 8, pp. 1472–1475. © Pleiades Publishing, Ltd., 2014.
Original Russian Text © L.B. Gulina, V.P. Tolstoy, 2014, published in Zhurnal Obshchei Khimii, 2014, Vol. 84, No. 8, pp. 1243–1246.

Reaction of Gaseous Hydrogen Fluoride with the Surface of Lanthanum Chloride Solution to Form $LaF_3 \cdot nH_2O$ Film and Microtubes Thereof

L. B. Gulina and V. P. Tolstoy

St. Petersburg State University, Universitetskii pr. 26, St. Petersburg, 198504 Russia
e-mail: l.gulina@spbu.ru

Received March 25, 2014

Abstract—We present the first study of the reaction of hydrogen fluoride fed from the air side of the air/$LaCl_3$ aqueous solution interface with lanthanum cations. The reaction yields a 0.5–1.5-μm $LaF_3 \cdot nH_2O$ surface film with hexagonal crystal structure, built of the ordered planar $LaF_3 \cdot nH_2O$ nanocrystals (the crystal thickness of 7–15 nm and surface area of 0.5–2.5 μm^2). The nanocrystals are oriented perpendicular to the interphase boundary, and their packing gets looser towards the solution side of the film. Upon drying in air, the $LaF_3 \cdot nH_2O$ film rolls up to form microtubes 20–100 μm in diameter and up to 2 mm long. The microtubes are likely formed due to the contraction forces developing upon drying in the lower, loosest part of the wet film.

Keywords: liquid–gas interface, film, microtube, nanosheet, lanthanum fluoride, tysonite

DOI: 10.1134/S1070363214080039

Preparation of one- and two-dimensional inorganic crystals is among topical issues of modern inorganic chemistry, because it opens up unique opportunities for creating promising functional materials [1, 2]. In particular, 2D crystals can be used to fabricate nano- and microtubes of metal oxides, sulfides, etc. [1, 3–5]. Much effort is being directed towards synthesis of nanosized metal fluorides, including lanthanum fluoride applied in development of F, O_2, and CO sensors [6], materials for superionic conductors [7], and luminophor scaffolds [8].

A number of procedures for synthesis of LaF_3 nanoparticles have been reported [8–14], including hydrothermal synthesis [9, 10], high-temperature fusion of $La(NO_3)_3$ with NH_4F [11], liquid solid solution process [12], microwave synthesis [13], and surfactant-assisted synthesis [14].

In the present work we developed a new, facile, liquid–gas process for synthesis of LaF_3 crystalline nanosheets. The process yields a film built of LaF_3 nanosheets at the surface of the aqueous solution. This approach was previously developed and applied [15, 16] to prepare $H_xMnO_2 \cdot nH_2O$ films. The outstanding feature of this procedure is that it allows preparation of inorganic nanofilms and microtubes under mild conditions (room temperature) and requires no sophisticated equipment, surfactant additives, or rigid scaffold.

Scanning electron microscopy (SEM) of the synthesized samples (Fig. 1) showed that the film formed at the aqueous solution–air (HF) interface consisted of a number of ordered nanosheets, being oriented predominantly perpendicular to the solution–air interface. The nanocrystals packing in the bottom part of the film (the solution side) was looser than that in the upper part. The microscopy study revealed that the nanosheets were 7–15 nm thick, and surface area of each nanosheet was of 0.5–2.5 μm^2 depending on synthesis conditions. The average thickness of the so formed nanocomposite film was of 0.5–1.5 μm.

In the course of drying in air, the film rolled up to form microtubes (Fig. 2).

X-ray spectral microanalysis showed that the microtube walls contained La and F atoms and no chloride ions (present in the starting $LaCl_3$ solution). According to the X-ray powder diffraction data (Fig. 3), crystal structure of the nanosheets forming the film corresponded to the hexagonal tysonite modification [17]. That was further confirmed by IR spectral data (Fig. 4): the IR spectrum contained a band at 352 cm^{-1} assigned to La–F stretching characteristic of the tysonite-like LaF_3 crystal [18]. IR absorption bands at 3400 and 1630 cm^{-1} were assigned to stretching and deformation vibrations, respectively, of O−H bonds in water.

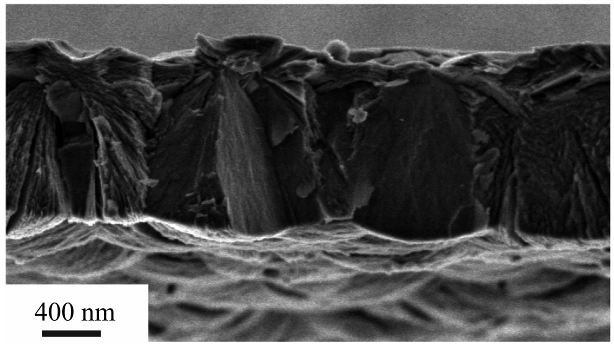

Fig. 1. SEM image of the cross-section of the synthesized LaF_3 film.

(a) (b)

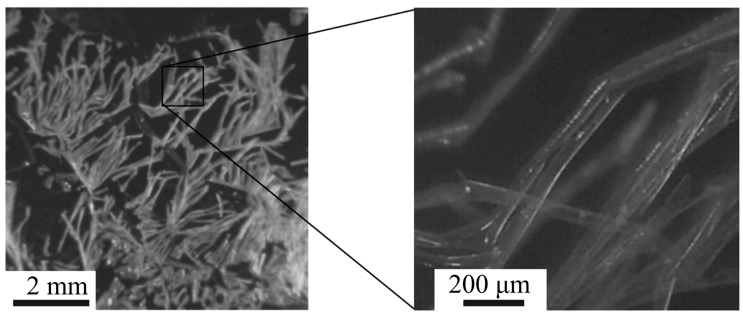

Fig. 2. Optical microscopy images of LaF_3 microtubes at (a) ×50 and (b) ×200 magnification.

The experimental observations suggested the following model of the oriented $LaF_3{\cdot}nH_2O$ nanosheets formation. The initially formed nanocrystals were oriented horizontally at the surface of the aqueous solution, they could be observed on top of the final film (Fig. 1). The nanocrystals somewhat blocked HF molecules from freely entering the lanthanum salt solution; HF transport into the solution was only possible through the gaps between the nanocrystals at the surface. Hence, the further formed crystals grew starting from the gaps predominantly perpendicular to the interface, and the packing density decreased towards the film bottom (solution) side. Upon drying of such gradient film, contraction forces developing due to water removal changed the planar geometry of the film to tubular (Fig. 5). Our experiments showed that such microtubes were 20–100 µm in diameter and 0.4–2 mm long.

EXPERIMENTAL

Aqueous solutions of $LaCl_3$ (“special pure” grade, 0.02–0.05 mol/L) and concentrated aqueous HF (“chemical pure” grade, Vekton, Russia) were used. All solutions were prepared using deionized water. Syntheses were performed as described elsewhere [15], in the steady-state mode. The $LaCl_3$ solutions were exposed to HF vapor during 10–60 min.

SEM images were obtained using the Zeiss Merlin scanning electron microscope at accelerating voltage of 2 kV. The film composition was determined using

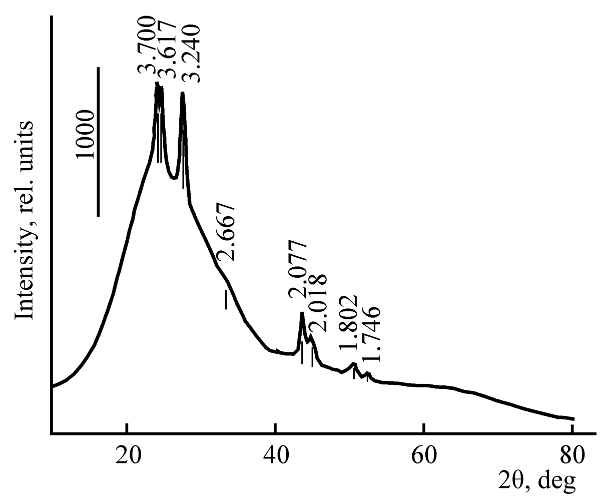

Fig. 3. X-ray diffraction pattern of LaF_3 microtubes.

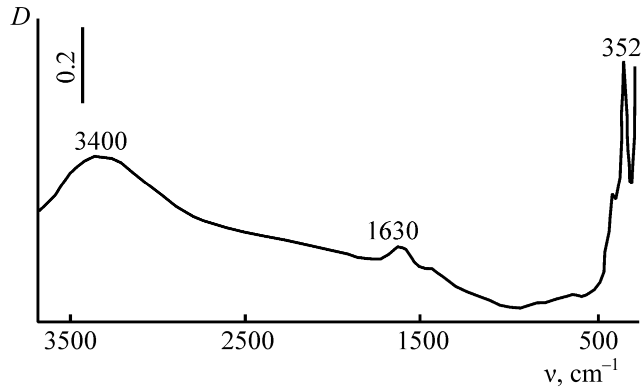

Fig. 4. Differential (the initial silicon surface as reference) FTIR spectrum of the LaF_3 film at the silicon support.

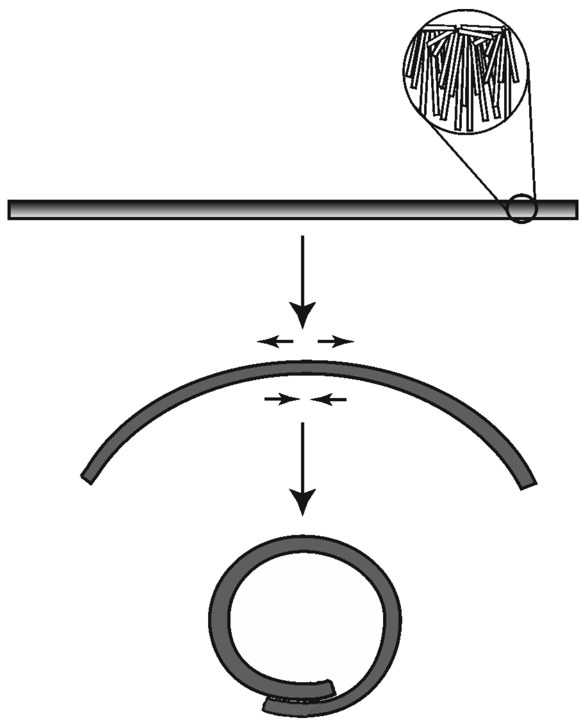

Fig. 5. Model of LaF_3 microtube formation upon drying of the anisotropic film (see text for details).

the Oxford Instruments INCAx-act energy dispersion analyzer at accelerating voltage of 10 kV. Optical microscopy images of LaF_3 microtubes were obtained using the PenScope digital microscope (×50 and ×200). FTIR spectra were recorded with the Bruker Vertex 70 spectrophotometer (50 scans). X-ray diffraction patterns were obtained using the Rigaku MiniFlex II diffractometer (CuK_α radiation).

Exposure of aqueous $LaCl_3$ to HF vapor yielded transparent solid surface film. To remove excess of the solution, the film was carefully transferred onto the surface of distilled water in a 300 mL beaker and incubated during 10–15 min. The transfer–incubation procedure was repeated three times. Then, the film was transferred onto monocrystalline silicon support, dried at room temperature, and studied with IR spectroscopy, scanning electron microscopy, X-ray spectral microanalysis, and X-ray diffraction. To remove any organic contaminants from the silicon support, it was washed with acetone, ultrasonicated at 60 W during 0.2 h immersed in the 3 : 7 mixture of 30 wt % H_2O_2 and conc. H_2SO_4 (“piranha” solution), and thoroughly washed with water prior to use.

ACKNOWLEDGMENTS

The synthesized samples were studied at the Resource Centers for X-ray Diffraction Studies and the Interdisciplinary Center for Nanotechnologies, St. Petersburg State University.

The work was financially supported by St. Petersburg State University (project no. 12.38.259.2014).

REFERENCES

1. Devan, R.S., Patil R.A., Lin J.H., and Ma, Y.R., *Adv. Funct. Mater.*, 2012, vol. 22, p. 3326. DOI: 10.1002/adfm.201201008.
2. Zhang, Q., Liu, Sh.-J., and Yu, Sh.-H., *J. Mater. Chem.*, 2009, vol. 19, p. 191. DOI: 10.1039/B807760F.
3. Rottler, A., Harland, M., Bro, M., Schwaiger, S., Stickler, D., Stemmann, A., Heyn, Ch., Heitmann, D., and Mendach, S., *Appl. Phys. Lett.*, 2012, vol. 100, p. 151104. DOI: 10.1063/ 1.4704185.
4. Huang, G. and Mei, Y., *Adv. Mater.*, 2012, vol. 24, p. 2517. DOI: 10.1002/adma.201200574.
5. Prinz, V.Ya., *Microelectr. Eng.*, 2003, vol. 69, p. 466. DOI: 10.1016/S0167-9317(03)00336-8.
6. Vijayakumar, M., Selvasekarapandian, S., Gnanasekaran, T., Fujihara, Sh., and Koji, Sh., *Appl. Surf. Sci.*, 2004, vol. 222, p. 125. DOI: 10.1016/j.apsusc.2003.08.002.
7. Ivanov-Shits, A.K. and Murin, I.V., *Ionika tverdogo tela* (Solid-State Ionics), St. Petersburg: Sankt-Peterb. Gos. Univ., 2000, vol. 1.
8. Gai, Sh., Li, Ch., Yang, P., and Lin, J., *Chem. Rev.*, 2014, vol. 114, p. 2343. DOI: 10.1021/cr4001594.
9. Hu, H., Chen, Zh., Cao, T., Zhang, Q., Yu, M., Li, F., Yi, T., and Huang, Ch., *Nanotechnology*, 2008, vol. 19, p. 375702. DOI: 10.1088/0957-4484/19/37/375702.

10. Sun, X., Zhang, Y.-W., Du, Y.-P., Yan, Zh.-G., Si R., You L.P., Yan Ch.-H., *Chem. Eur. J.*, 2007, vol. 13, p. 2320. DOI: 10.1002/chem.200601072.
11. Zhang, J., Sui, N., Chen, D., and Hong, G., *J. Nanopart. Res.*, 2010, vol. 12, no. 1, p. 161. DOI: 10.1007/s11051-009-9590-5.
12. Wang, X., Zhuang, J., Peng, Q., and Li, Y., *Nature*, 2005, vol. 437, no. 7055, p. 121. DOI: 10.1038/nature03968.
13. Jacob, D.S., Bitton, L., Grinblat, J., Felner, I., Koltypin, Yu., and Gedanken, A., *Chem. Mater.*, 2006, vol. 18, p. 3162. DOI: 10.1021/cm060782g.
14. Wang, G., Peng, Q., and Li, Y., *Acc. Chem. Res.*, 2011, vol. 44, p. 322. DOI: 10.1021/ar100129p.
15. Tolstoi, V.P. and Gulina, L.B., *Russ. J. Gen. Chem.*, 2013, vol. 83, p. 1635. DOI: 10.1134/S1070363213090016.
16. Tolstoy, V.P. and Gulina, L.B., *J. Nano Electron. Phys.*, 2013, vol. 5, p. 01003.
17. *Database PDF-2 of Int. Centre for Diffraction Data*; Card 01-076-0510.
18. Tolstoy, V.P., Chernyshova, I.V., and Scryshevsky, V.A., *Handbook of Infrared Spectroscopy of Ultrathin Films*, New York: Wiley-Interscience, 2003, p. 676.